



On the Unusual Temperature Dependence of Kaolinite Intercalation Capacity for N-methylformamide

Fevronia T. Andreou · Eirini Siranidi ·
Arkadiusz Derkowski ·
Georgios D. Chryssikos

Accepted: 2 January 2023 / Published online: 17 January 2023
© The Author(s) 2023

Abstract Many kaolinites are known to exhibit limited intercalation capacity which affects their usage. Some reports have linked this lack of reactivity to particular structural features or to slow kinetics; others recommended increasing intercalation temperature as a remedy. The purpose of the current study was to investigate systematically the N-methylformamide (NMF) intercalation capacity of three kaolinites differing in layer stacking order (KGa-1b, KGa-2, and Imerys Hywite Alum) in the 5–150°C temperature range. Near-infrared spectroscopy (NIR) was employed to record the full kinetics of intercalation in closed systems with excess NMF. Increasing intercalation temperature accelerated the reaction, but the NMF uptake decreased and eventually vanished. Complementary thermogravimetric analysis (TGA) confirmed this unexpected trend. All kaolinites

exhibited the same behavior, but the amount of inert material was in the order of their stacking-fault concentration at all temperatures: KGa-2 > Hywite > KGa-1b. Subjecting the samples to stepwise temperature changes showed that, once intercalated, the NMF could not deintercalate and was removed from equilibrium with the surrounding fluid. Thus, intercalation capacity was not a unique feature of the material because it depended on thermal history. As stacking order and thermal history had no detectable effect on the NMF-hosting environment, the unusual temperature dependence was attributed tentatively to the adverse effect of temperature on the adsorption of NMF on the edges of the crystallites, which is a prerequisite for intercalation.

Keywords Intercalation capacity · Kaolinite · N-methylformamide · Near-infrared spectroscopy (NIR) · Thermogravimetric analysis (TGA)

Associate Editor: Jana Madejová

Supplementary Information The online version contains supplementary material available at <https://doi.org/10.1007/s42860-023-00217-9>.

F. T. Andreou · E. Siranidi · G. D. Chryssikos (✉)
Theoretical and Physical Chemistry Institute, National
Hellenic Research Foundation, 48 Vas. Constantinou Ave,
11635 Athens, Greece
e-mail: gdchryss@eie.gr

A. Derkowski
Institute of Geological Sciences, Polish Academy
of Sciences, Senacka 1, 31-002 Krakow, Poland

Introduction

Certain molecules such as hydrazine, DMSO, small amides, K-acetate, etc., are known to intercalate spontaneously the interlayer space of kaolinite (a 1:1 dioctahedral clay mineral) shifting its X-ray diffraction (XRD) 001 reflection from ~7.2 to 10–14 Å (Kloprogge, 2019; Lagaly et al., 2006). A common finding in kaolinite intercalation studies is that, regardless of the type of guest molecules,

there is a population of kaolinite that is resistant to intercalation (Lagaly et al., 2006; Rausell-Colom & Serratos, 1987). The intercalation capacity (otherwise referred to below as ‘yield’) of kaolinite for particular guest molecules should be considered at virtually infinite reaction time. The amount of intercalation-recalcitrant material has been considered as an intrinsic, but poorly understood, property of the kaolin material. This property determines the value of kaolinite in many technological applications (e.g. Dedzo & Detellier, 2016; Seifi et al., 2016). Experimentally, the limited intercalation capacity of a given kaolinite should not be confused with the rate of its intercalation, despite the fact that both properties may exhibit a similar dependence on kaolinite type (Rausell-Colom & Serratos, 1987).

Both the crystallite size and the stacking order of kaolinite have been considered as determining the intercalation capacity. Distinguishing between the two is not straightforward because crystallite size is often related to crystal imperfection (Gomes, 1982; Rausell-Colom & Serratos, 1987). There is evidence that high-defect kaolinites have low intercalation yields, but low-defect samples with little tendency for intercalation are also known (Frost et al., 2002; Uwins et al., 1993). Smaller kaolinite particles intercalate less than their larger counterparts, if at all (Lagaly et al., 2006 and references therein). For example, the intercalation yield of nine kaolinites subjected to the same intercalation agent (N-methylformamide, NMF) and protocol were measured by Uwins et al. (1993). Bulk kaolinites exhibited yields between ~70 and 95%, whereas their finer fractions demonstrated systematically smaller yields, as low as ~30%. According to the literature, particle size seems to be the primary determinant of intercalation capacity. The low reactivity of kaolinite is often attributed to the fact that smaller particles display slow kinetics of intercalation (Deng et al., 2002; Lagaly et al., 2006; Uwins et al., 1993; Weiss et al., 1970). Recently, Fashina and Deng (2021) suggested that, for the same size fraction, increasing stacking disorder decreases reactivity toward K-acetate intercalation and NaOH dissolution.

All the aforementioned literature studies of intercalation capacity were based on XRD determinations of the relative intensity of the 001 reflections from pristine and intercalated interlayers. The accuracy of these determinations has been

questioned by a recent real-time study of NMF intercalation by XRD and near-infrared spectroscopy (NIR), cross-verified by thermal analysis (Andreou et al., 2021). The fraction of KGa-1b and KGa-2 kaolinites resisting intercalation by NMF was much greater than originally estimated by XRD (20–25% and 55–60%, instead of 7 and 23%, respectively). This difference was attributed to the erroneous assumption that the Lorenz polarization and structure factors of the two basal reflections in the XRD were equal (c.f. Hach-Ali & Weiss, 1969). The NIR spectroscopic methodology introduced by Andreou et al. (2021) is particularly convenient for recording dense kinetic data of sealed kaolinite/NMF mixtures containing excess NMF and reacting over long times (several days) as a function of temperature. These authors demonstrated that, owing to changes in mechanical anharmonicity, NIR is capable of distinguishing a minority of intercalated NMF molecules with dangling N–H bonds from the majority of H-bonded NMF present in the surrounding liquid or on the external aluminol surfaces of the crystallites. Further, NIR is capable of detecting the intercalated molecules by their local chemical environment without requiring long-range structural coherence, as in XRD.

Intercalation is typically a slow process, frequently accelerated by increasing temperature (Lagaly et al., 2006). If the amount of non-intercalated kaolinite were controlled by slow kinetics, as suggested in the literature (e.g. Deng et al., 2002), it could be reduced or even removed at higher temperatures. Relevant variable-temperature data of NMF intercalation capacity in the XRD-based literature are scarce and do not support a strong temperature dependence (Hach-Ali & Weiss, 1969; Makó et al., 2019). This lack of temperature dependence may, however, be due to the overestimation of intercalation capacity by the XRD intensity ratio method, as proposed by Andreou et al. (2021). The present investigation aimed to study the effect of temperature on kaolinite intercalation capacity for NMF in order to examine the hypothesis that the low uptake of guest molecules is determined by slow kinetics. This was done by employing the toolbox developed by Andreou et al. (2021) to study the intercalation of NMF in the interlayer of three different kaolinites over a broad temperature range (5–150°C).

Materials and Methods

Materials

Three kaolinite samples were considered in this study: KGa-1b and KGa-2 obtained from the Source Clays Repository of The Clay Minerals Society, and Hywite Alum raw kaolinite from Imerys, UK. The latter was a sample included in recent studies by Drits et al. (2019, 2021) and kindly provided by V.A. Drits. According to these authors, Hywite Alum (hereafter Hywite) is a “ball clay” from Devon, UK. It is ~85% pure with ~6% organic matter and minor admixtures of quartz (~5%), illite (3%), Fe₂O₃ (<1%), and anatase (<1%). For the removal of adsorbed H₂O, the as-received samples were dried at 100°C for 2 h and kept sealed. N-methylformamide (NMF) (99% purity), obtained from Sigma-Aldrich (St Louis, Missouri, USA), was also dried using 4 Å molecular sieves.

The kaolinite samples studied differ in their layer stacking order, as reflected in the XRD patterns (Hinckley index of the order of 1.1, 0.6, and 0.3 for KGa-2, Hywite, and KGa-1b, respectively; Fig. S1 in Electronic Supplement). According to Drits et al. (2021), who successfully simulated the XRD patterns using a physical mixture binary system, KGa-2, Hywite, and KGa-1b samples contain 4, 18, and 37%, respectively, of the so-called high-order kaolinite (HOK) population containing almost exclusively t_1 ($-a/3$) vector layer displacements. The remaining population is a low-order kaolinite (LOK) modeled using a random interstratification of enantiomorphic t_1 ($-a/3$) and t_2 ($-a/3+b/3$) layer displacements with roughly 0.6 to 0.4 proportions (Sakharov et al., 2016).

Near-infrared Spectroscopy

Approximately 2 g mixtures of kaolinite with excess NMF were prepared in ~5 mL glass vials using pre-dried stock materials. The kaolinite/NMF mixtures were 1:1 by mass in the case of KGa-1b or KGa-2, and 1:0.7 for Hywite, to achieve the same paste consistency. Real-time NIR spectra of all kaolinite/NMF mixtures in the 30–100°C range were measured using the procedure described by Andreou et al. (2021). The KGa-1b series at 30, 45, and 70°C and their KGa-2 counterparts at 30 and 45°C were taken from Andreou et al. (2021).

The NIR spectra were measured on a diffuse reflectance infrared Fourier transform instrument (Vector 22N by Bruker, Ettlingen, Germany) by means of a 1.5 m long fiber optic bundle probe (9000–4000 cm⁻¹). All NIR spectra were acquired as averages of 100 scans for KGa-1b and KGa-2 and 400 scans for Hywite at a resolution of 4 cm⁻¹ ($\Delta\nu = 2$ cm⁻¹). Fourier transform was computed using a Blackman-Harris 3-term apodization. Post-processing of the NIR absorbance spectra was based on subroutines of the Bruker *Opus* software and involved the calculation of the 2nd derivatives (Savitzky-Golay algorithm, 9-point smoothing), as well as vector normalization. The latter is a normalization procedure applied to a group of spectra, which are converted so that their vector norm over a chosen frequency range (i.e. the sum of the intensities squared) equals unity. For the vectorial definition of a spectrum and its applications in vibrational spectroscopy, see Chryssikos and Gates (2017).

Immediately after the mixing of the sample, the vial was attached to the tip of the probe, sealed and immersed in a thermostatic H₂O or silicone oil bath, depending on temperature (30–100±0.5°C). Periodic spectral measurements were initiated immediately after immersion. The temporal resolution was between 2 and 30 min, depending on temperature.

Low-temperature (5°C) intercalation was performed ex situ. The sealed samples were kept refrigerated for 3 months and measured through the bottom of the glass vial using the NIR probe at frequent intervals, after brief equilibration at room temperature.

Additional high-temperature intercalation experiments at 125 and 150°C were performed in a laboratory oven, without NIR monitoring. After allowing for sufficient reaction time at the desired temperature in a sealed vial, the product was evaluated by NIR spectroscopy at room temperature. Intercalation experiments at 30 and 100°C were performed at least in duplicate.

Thermogravimetric Analysis

At the end of the intercalation experiments, ~100 mg of the intercalates were rinsed with 1,4-dioxane to remove excess liquid NMF (Tunney & Detellier, 1996) and air-dried at ambient temperature for 2–3 h. Then, 10±1 mg of the air-dried material was subjected to thermogravimetric analysis (TGA) on two instruments: Q500 and Discovery by TA Instruments (New Castle, Delaware, USA), located in the Athens and Krakow

laboratories, respectively. The samples were scanned from room temperature to 800°C at 10°C/min under dry N₂ purging (60 mL/min).

Results

Temperature-compensated Proxy of NMF Intercalation

The first overtone of the NH stretching fundamental mode ($2\nu\text{NH}$ and νNH , respectively) of intercalated NMF was the main NIR proxy introduced by Andreou et al. (2021) to monitor the amount of intercalated NMF. The use of this proxy was justified by its good separation from the corresponding mode of excess liquid NMF, especially when 2nd derivatives are employed, as well as by its remarkably stable position and width. The latter were independent of reaction progress and kaolinite type at any temperature studied (Andreou et al., 2021), a finding which is now extended to include Hywite, in addition to KGa-1b and KGa-2 (Fig. 1). Clearly, the NMF molecules probed the same interlayer environment in all three kaolinites and, within the sensitivity of the NIR experiment, this environment did not change during intercalation. As a result, if the temperature is fixed, the intensity of the $2\nu\text{NH}$ probe band is well correlated with the degree of NMF intercalation, regardless of the kaolinite host.

When comparing $2\nu\text{NH}$ intensities from spectra measured at different temperatures, the temperature dependence of the proxy band is no longer negligible. One way to study the temperature dependence of the kaolinite/NMF spectra without affecting the degree of intercalation is by subjecting an infinitely intercalated sample to temperature variations. For this purpose, a sealed KGa-1b/NMF paste (1:1 by mass) was left to intercalate for 3 months at ambient temperature to reach its maximum degree of intercalation, and then adapted to the NIR optical fiber probe. The as-assembled reactor and sample were introduced in a thermostatic bath and stepwise heated (and subsequently cooled) from 30 to 80°C (and back to 30°C), every 10°C.

The broadening of the $2\nu\text{NH}$ band upon increasing temperature from 30 to 80°C caused a significant decrease in the 2nd derivative intensity accompanied

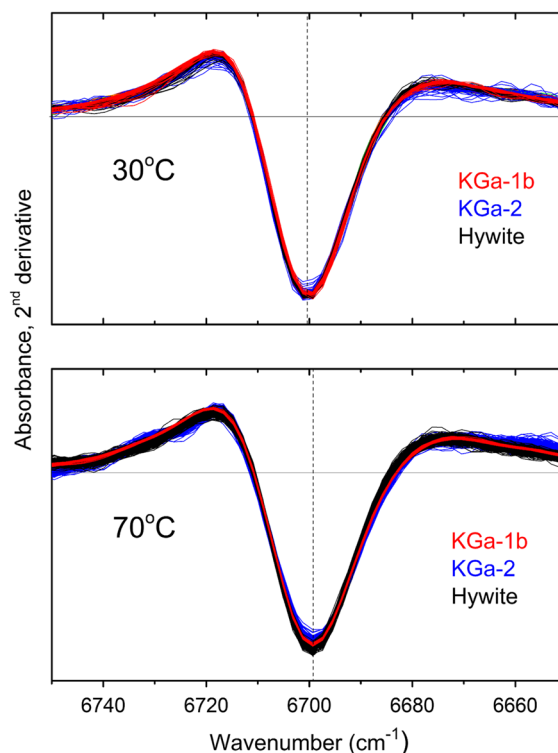


Fig. 1 Intensity-normalized $2\nu\text{NH}$ 2nd derivative spectra for KGa-1b (red), KGa-2 (blue), and Hywite (black) during intercalation with NMF at 30°C (upper) and 70°C (lower). Approximately 50–100 spectra per sample are overlain in each panel

by a slight red-shift of its position by $\sim 1\text{ cm}^{-1}$ (Fig. 2, lower). The strong $2\nu\text{OH}$ band of the inner OH groups, which was nearly unaffected by progressing intercalation (Andreou et al., 2021), also exhibited reduced intensity and minor shifting upon heating from 30 to 80°C (Fig. 2, upper). As temperature-induced changes affected both overtone bands similarly, their relative intensity $2\nu\text{NH}/2\nu\text{OH}$ was found to be independent of temperature within a narrow experimental error, however (Fig. S2). The same behavior and similar relative intensities were obtained for KGa-2 and Hywite. A temperature-independent semi-quantitative proxy of the actual NMF uptake could, therefore, be obtained by normalizing the 2nd derivative intensity of the $2\nu\text{NH}$ band to that of its $2\nu\text{OH}$ counterpart. For practical reasons, this was done by performing a vector-normalization of the derivative spectral intensities (see Materials and Methods) over the $2\nu\text{OH}$ frequency range (7100–7025 cm^{-1}) before

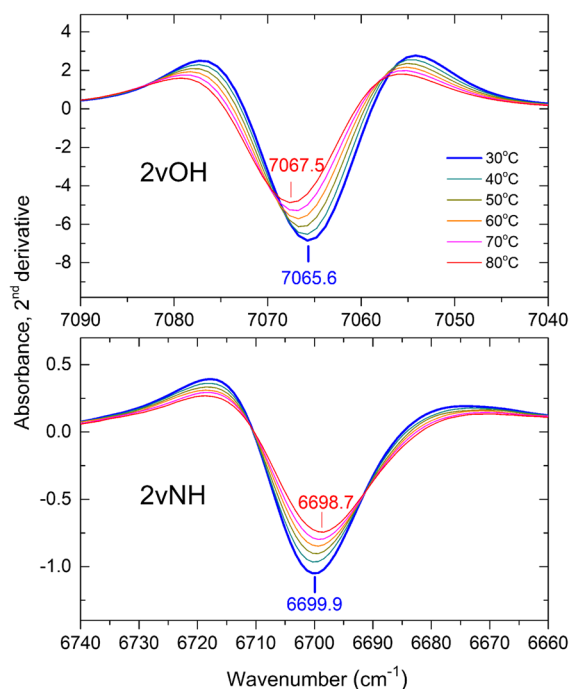


Fig. 2 Dependence of the 2νNH (lower) and inner 2νOH modes (upper) of a KGa-1b/NMF sample at its maximum intercalation after 3 months, as seen by the 2nd derivatives upon increasing temperature from 30 to 80°C

recording the intensity of the 2νNH (Fig. 3). The application of this mathematical pre-treatment to the spectra of samples intercalated at various temperatures is illustrated in Figs. S3 and S4. This treatment did not change the shape of the sigmoids reported by Andreou et al. (2021) but enabled for the first time the NIR assessment of the relative degree of intercalation at various temperatures.

Effect of Temperature on the Intercalation Capacity of Kaolinite

The normalized 2νNH intensity proxy described in the previous section enabled the semi-quantitative assessment of the sigmoidal NMF intercalation kinetics of the three kaolinites as a function of temperature (5–100°C, Fig. 4). After 3 days at 30°C the proxy took the values of 0.074, 0.063, and 0.043 for KGa1-b, Hywite, and KGa-2, respectively. These values scaled very well (rule-of-thumb factor of x10) with the NMF uptakes calculated from the relative decrease of the 001 reflection intensity of pristine KGa-1b and KGa-2 at ambient

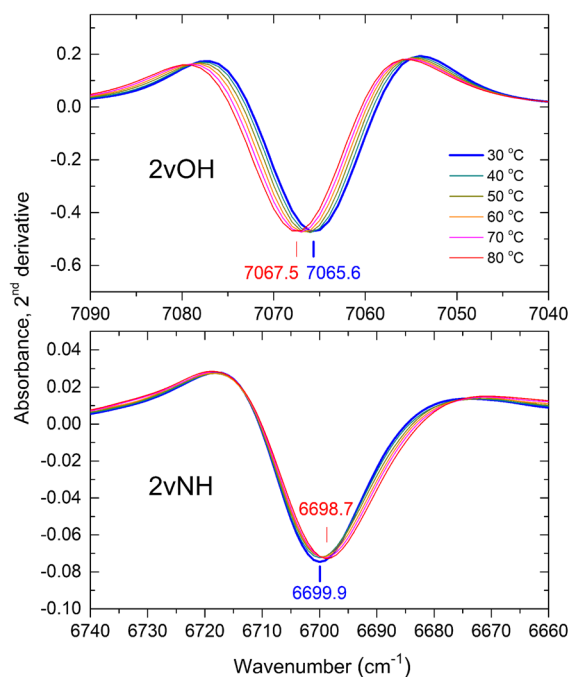


Fig. 3 Same as Fig. 2, following the vector-normalization of the derivative spectra over the full range of the 2νOH band (7100–7025 cm⁻¹). For details, see text

temperature (0.73 ± 0.02 and 0.44 ± 0.02 , respectively, Andreou et al., 2021). Hywite appeared to be intermediate between KGa-1b and KGa-2 in terms of final NMF uptake at 30°C (Fig. 4). Upon increasing temperature, the sigmoids of all kaolinites maintained approximately their shape and shifted to shorter times, as expected, but underwent a reduction in the final plateau intensity. This reduction suggested a remarkable decrease in the NMF uptake: from 5 to 100°C the relative drop in the intercalation capacity of KGa-1b was ~40%, compared to ~70% for Hywite, and ~80–90% for KGa-2. Intercalation of NMF in KGa-2 at 100°C was so suppressed that it was hardly detected (Fig. 4).

The final samples of each NIR run, as well as the final samples of runs at 125 and 150°C which were not monitored by NIR, were rinsed with 1,4-dioxane to remove excess liquid NMF (Tunney & Detellier, 1996) and dried at ambient conditions. The as-produced intercalated powders were subsequently studied by TGA (Fig. 5). The degree of intercalation of the dried powders was determined by both the aforementioned NIR relative intensity method, as well as from the mass loss in the 50–300°C range, in comparison to the

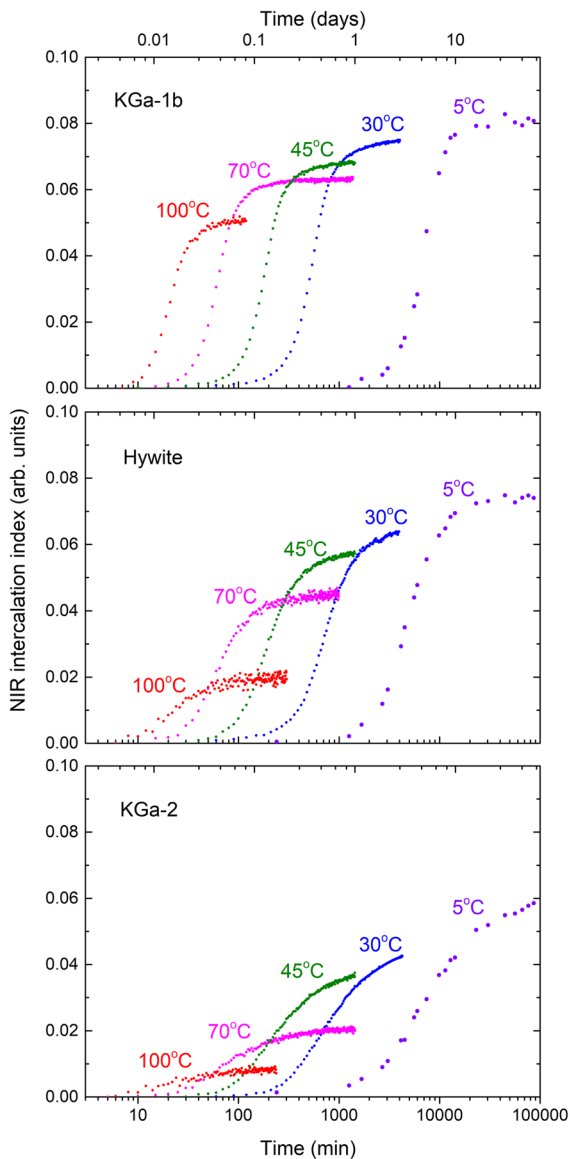


Fig. 4 Semiquantitative NIR intercalation kinetics at various temperatures from 5 to 100°C of KGa-1b/NMF (upper), Hywite/NMF (middle), and KGa-2/NMF (lower). The amplitudes of the 2nd derivative $2\nu_{\text{NH}}$ mode at 6700 cm^{-1} are plotted as a function of time, following vector-normalization over the $2\nu_{\text{OH}}$ range as in Fig. 3

kaolinite dehydroxylation loss in the 300–800°C range (Adams, 1978; Xie & Hayashi, 1999, Fig. 6). The latter determination involved normalizing the TGA traces to the % mass loss at 300°C and correcting for the purity of kaolinite (14% mass loss due to dehydroxylation). The low-temperature loss event normalized on the

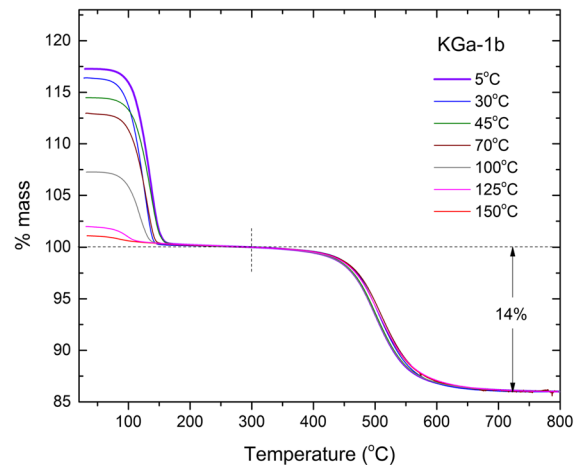


Fig. 5 TGA diagrams of KGa-1b/NMF slurries intercalated at various temperatures in the 5–150°C range, after washing with dioxane. The dehydroxylation losses (~13.5%) were normalized to 14% to represent 100% pure substrate

dehydroxylation of kaolinite was attributed to the loss of NMF and led to an estimate of the degree of intercalation by assuming that full intercalation corresponds to 2 NMF molecules per unit cell (Adams, 1979), i.e. 22.9 g NMF per 100 g kaolinite, as in Andreou et al. (2021). Full TGA data before and after the aforementioned normalization procedure on all kaolinites and temperatures investigated can be found in the Electronic Supplement (Figs. S5 to S7).

The two determinations of the degree of NMF intercalations were based on different assumptions, exposed to different sources of error and produced slightly different, albeit highly correlating, results (Fig. 6). For example, in all samples treated at $\geq 125^\circ\text{C}$, TGA indicated non-zero mass loss, contrasting with NIR. This mass loss may well originate from micropore-adsorbed, non-intercalated amide because it was not accompanied by the characteristic 6700 cm^{-1} sharp NH overtone of intercalated NMF. Yet, both the NIR and TGA methods proved independently that the intercalation capacity of all kaolinites investigated decreased with increasing temperature and that intercalation practically stopped at temperatures in the 125–150°C range. The intercalation capacity vs. temperature curves of the three kaolinites were similar in shape within error. At any temperature, the intercalation capacity decreased in the order KGa-1b > Hywite > KGa-2 due to the progressive shift of the curves to lower temperatures.

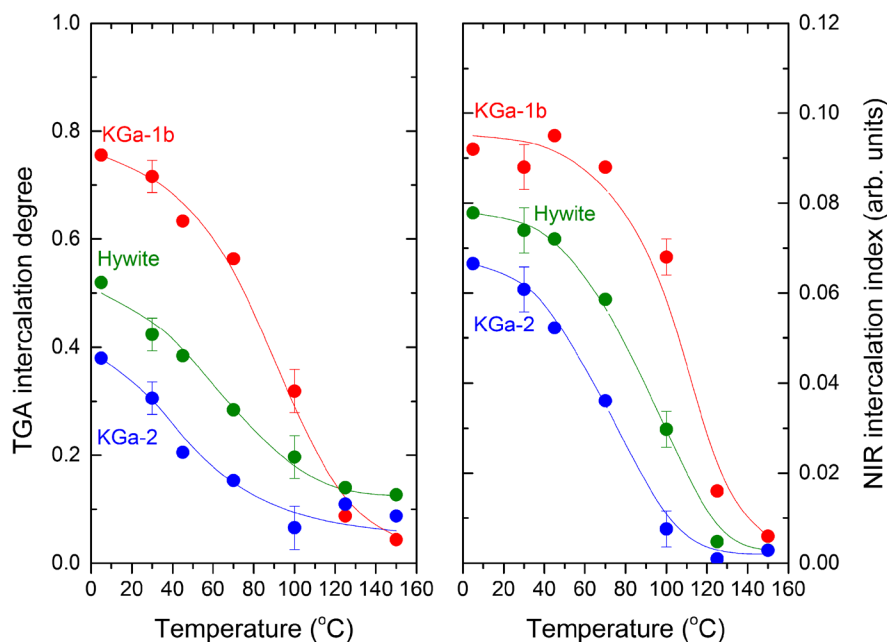


Fig. 6 NMF intercalation capacity of the three kaolinites investigated as a function of intercalation temperature, estimated by TGA (left) and NIR (right) after rinsing the samples with dioxane. Lines are used to guide the eye. Error bars represent the average cumulative effect of duplicate runs and dioxane treatment

Response of Intercalation Capacity to Temperature Changes

The unusual effect of temperature on intercalation capacity was further investigated by subjecting sealed kaolinite/NMF samples to stepwise temperature changes under real-time NIR monitoring. For example, a sealed KGa-2/NMF sample was left to intercalate at 70°C for 1 day (~24 h), then transferred to a 45°C bath for 1 day, and to a third bath at 30°C for a further day (Fig. 7). Due to its small mass, the temperature equilibration of the sealed sample between baths was instantaneous. After 1 day at 70°C, intercalation had reached a clear plateau and the reaction appeared stalled. Switching the temperature to 45°C caused the revival of the reaction and increase in the intercalation yield. Next, the decrease in temperature to 30°C triggered an additional NMF uptake process (Fig. 7). The uptakes of the 45 and 30°C segments extrapolated to those of the corresponding single-temperature kinetics for all kaolinites investigated.

The reversibility of the reaction was tested as follows: KGa-2 intercalated at 70°C for 1 day was transferred to 30°C for the next 3 days and then returned to

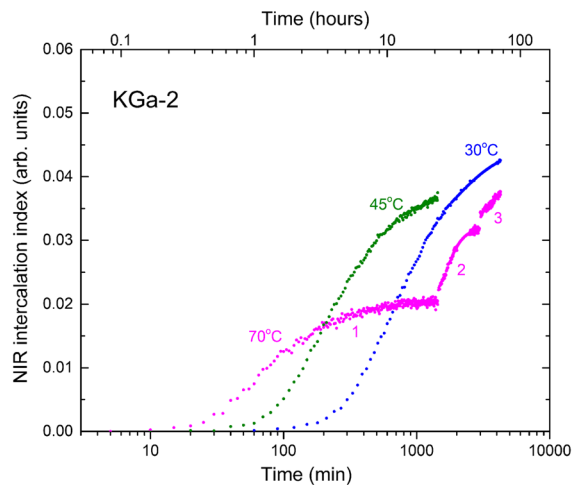


Fig. 7 Semiquantitative NIR intercalation kinetics of KGa-2/NMF at 70°C (1), with subsequent insertion at 45°C (2), and then at 30°C (3). The single-temperature kinetics are depicted for comparison

70°C for 1 further day. During all three stages, intercalation was monitored in situ by the normalized 2vNH intercalation index (Fig. 8). The first stage at 70°C

resulted in the expected fast, but incomplete, NMF uptake (Fig. 8a, c.f. Fig. 7). Decreasing temperature from 70 to 30°C caused a second intercalation step which eventually doubled the original 70°C uptake of NMF (Fig. 8b), as expected from Fig. 7. The return of the system to 70°C caused no detectable decrease of intercalated NMF, however (Fig. 8c). During the two 70°C segments, the $2\nu_{\text{NH}}$ band maintained the same position and width (data not shown, c.f. Fig. 1). Maintaining this sample at 70°C for an additional period of 6 days and measuring its NMF uptake *ex situ* during this period provided no evidence for deintercalation. This meant that the NMF which was successfully intercalated during the 30°C step became trapped in the interlayer upon return to 70°C and did not deintercalate.

Discussion

Temperature Dependence of Intercalation Capacity

Despite the fact that NMF is a common probe molecule for studying the systematics of kaolinite intercalation (Hach-Ali & Weiss, 1969; Makó et al., 2019; Olejnik et al., 1971a; Uwins et al., 1993), the present

study provided the first solid demonstration of the temperature effect on intercalation capacity. No such effect of temperature (7–65°C) was reported in the early study of Hach-Ali and Weiss (1969) on a kaolinite from Hirschau, Bavaria. Neither did Makó et al. (2019) report any change in kaolinite intercalation capacity upon increasing the reaction temperature from 20 to 60°C, although a small decrease by ~5% may be seen in their data. Note that the latter authors quantified the degree of intercalation by the incorrect relative XRD intensity method which assumes that the 001 reflections of pristine and intercalated kaolinite are of equal Lorentz polarization and structure factors (c.f. Andreou et al., 2021). Uniquely, a study by Kovács and Makó (2016) reported that cooling well below 0°C not only improved the intercalation capacity of kaolinite for ammonium acetate, but also accelerated the rate of intercalation!

The current investigation demonstrated for the first time by means of NIR spectroscopy and TGA that the kaolinite intercalation capacity or, conversely, the fraction of kaolinite resistant to intercalation by NMF, is heavily dependent on temperature. The spectroscopic evidence was obtained by recording the full kinetic curves at all temperatures, thereby excluding the

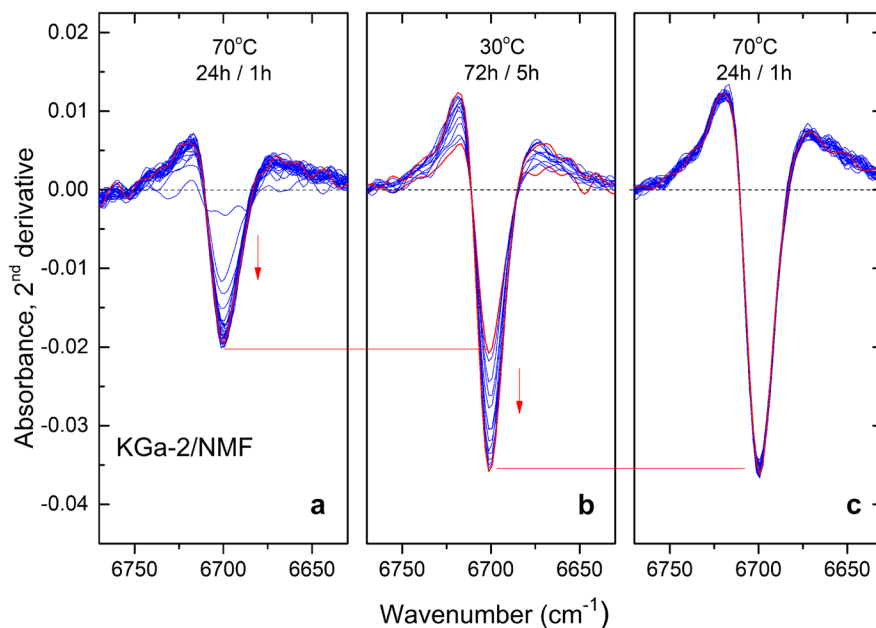


Fig. 8 Amplitude evolution of the 2nd derivative ($\Delta\nu = 2 \text{ cm}^{-1}$, 9-point smoothing) of the $2\nu_{\text{NH}}$ band normalized to that of the inner-hydroxyl $2\nu_{\text{OH}}$ band in KGa-2/NMF. Three sequential experiments are shown: **a** 24 h intercalation at 70°C, followed by **b** 72 h at 30°C, and **c** another 24 h at 70°C

possibility that incomplete intercalation was due trivially to an inadequate observation-time window. Surprisingly, intercalation capacity decreased with increasing reaction temperature, despite the expected reaction acceleration, and could be essentially eliminated at temperatures in the 125–150°C range (NMF boiling point: 183°C). Counterintuitively and unlike common practice (e.g. Lagaly et al., 2006), increasing temperature is not the way to improve intercalation capacity.

All three different kaolinites investigated displayed a similar temperature dependence of their intercalation capacity, suggesting that the underlying mechanism is common and independent of their individual characteristics. All three were nearly inert to NMF intercalation at high temperatures and tended monotonically towards full capacity upon decreasing temperature. As a result, the maximum intercalation capacity was observed at the lowest temperature investigated (5°C). Full capacity was not observed, perhaps because the proximity of the freezing point of NMF (−4°C) and the very slow intercalation rate both set a practical limit. The slopes of decreasing capacity with increasing temperature were similar within error, but the curves of the three kaolinites were shifted so that, at any temperature investigated, the capacities were in the order KGa-1b > Hywite > KGa-2. Significant amounts of kaolinite were inert at the lowest temperature in this study (5°C). Allowing for some losses of intercalated NMF due to the dioxane rinsing that preceded the TGA determinations, at least 20% of KGa-1b, 50% of Hywite, and 60% of KGa-2 were resistant to NMF intercalation (Fig. 6).

Correlation with Mineral Structure

A common underlying mechanism should account for both the decrease in intercalation capacity with increasing temperature and the large differences in the intercalation-resistant fraction observed at any temperature. The mechanism should comply with the conclusions of Andreou et al. (2021), who proved that intercalation displayed a binary behavior with the crystallites switching between the pristine and fully intercalated states. As the original material presents a distribution of crystallites, the distribution of intercalation events in time is lognormal and leads to apparent sigmoidal kinetics.

The present results suggested that the intercalation capacity of any of the three kaolinites investigated

was not solely dependent on temperature, but also on thermal history. Upon cooling a kaolinite/NMF mixture pre-intercalated at high temperature, the intercalation capacity increased. On the contrary, heating a low-temperature pre-intercalated kaolinite did not result in decreased capacity (Fig. 8). Once the interlayer became intercalated it acted as an NMF sink and, in a closed system, the interlayer NMF was not in equilibrium with that in the surrounding liquid. This is an important feature of the mechanism sought.

The interlayer interactions of the intercalated phase are determined by the weak H-bonding between the N–H bond and the adjacent siloxane sheet (Adams, 1979). Any differentiation of the kaolinites investigated in terms of these bonding interactions ought to be reflected in changes in the position and width of the $2\nu_{\text{NH}}$ mode. No such changes were observed and the proxy band was remarkably independent of the kaolinite studied (Fig. 1), which was fully consistent with the XRD-based conclusion by Andreou et al. (2021) for the binary state (pristine or fully intercalated) of the NMF-treated kaolinite. The present data indicated that the proxy was also independent of thermal history. The relatively small amount of material originally intercalated at 70°C and the much larger amount intercalated at 30°C and then equilibrated at 70°C were indistinguishable in terms of interlayer structure and bonding.

In discussing the limited intercalation capacity of the finer kaolinite particles, Deng et al. (2002) proposed that the misfit between the linked tetrahedral and octahedral sheets of kaolinite caused the accumulation of structural stress in the H-bonding pattern of the interlayer, which was thought to be released when the guest-molecules entered into the interlayer space. The magnitude of the original stress in pristine kaolinite was, therefore, considered to control intercalation. Although this stress may be temperature dependent, the stability of the kaolinite structure in nature suggests that the massive switching-off of intercalation over a relatively narrow (for a solid mineral) temperature range could not be attributed to the temperature dependence of the layer or interlayer structure. Instead, it should correspond to the range of change in liquid properties (NMF freezing point −4°C, boiling point 183°C) and liquid–mineral edge interactions.

Qualitatively, the portion of reactive material at any temperature $\leq 100^\circ\text{C}$ was in the order

KGa-1b > Hywite > KGa-2. This order followed the amount of the low-defect, high-order kaolinite (HOK) phase in the samples which was 37, 18, and 4%, respectively (Drits et al., 2021; Sakharov et al., 2016). The trend appeared to support the interpretation by Fashina and Deng (2021) who linked the limited intercalation capacity (as well as the low reactivity toward alkaline leaching) with the stacking disorder of the kaolinite layers. No simple quantitative correlation between intercalation capacity and the high-ordered fraction was found, however. In fact, KGa-1b with only 38% HOK content achieved an intercalation capacity of almost 80% at ambient temperature, ‘pushing’ the intercalation capacity of the many kaolinites with HOK > 37% (e.g. Drits et al., 2021) into a higher, but very narrow range (80–100%). Any correlation between stacking order and intercalation capacity would be premature without the study of samples with greater HOK contents.

Based on the discussion above, the variability in NMF intercalation capacity and its pronounced temperature dependence cannot be explained by the kaolinite layer stacking differences alone nor by the response of the kaolinite structure to temperature. The partition of NMF molecules between the liquid and the liquid–solid interface as well as its temperature dependence seem, instead, to provide a more plausible explanation for the observed experimental trends. The presence of the surrounding fluid is of paramount importance for maintaining the interlayer intercalated as in Fig. 8, because thermal deintercalation is very common and relatively fast in open systems (e.g. Adams, 1978; Frost et al., 1999, 2000; Kristóf et al., 1999; Olejnik et al., 1968, 1971a, 1971b; Ruiz Cruz & Franco, 2000; Zhang et al., 2015, 2017). The adsorption of NMF molecules on the edges of the crystallites provides the critical number of ‘wedges’ which is necessary for expanding the interlayer, according to the model of Weiss et al. (1981) (see also Lagaly, 1984). Edge adsorption seems to govern other stacking-order-dependent kaolinite reactions, such as the alkaline hydrolysis studied by Fashina and Deng (2021). The mobility of the NMF in the liquid increases with increasing temperature (thereby accelerating the reaction), but its sticking coefficient on the edges may be decreasing (thereby decreasing the efficiency of wedging).

Conclusions and Perspectives

Three kaolinites with intermediate or large fractions of stacking defects, KGa-1b, KGa-2, and Hywite, were all found to exhibit a significant temperature dependence of their intercalation capacity for N-methylformamide (NMF). Intercalation accelerated with increasing temperature, as expected, but intercalation capacity decreased and eventually disappeared. These findings were based on the dense NIR recording of the full kinetics of sealed kaolinite/NMF slurries in the 5–150°C range, accompanied by TGA analysis of the final products. Whether this type of behavior is generally observed with all types of guest molecules or solely with NMF is unknown.

The proportion of the intercalated material at any given temperature (below 100°C) was dependent on the kaolinite studied and followed the order: KGa-1b > Hywite > KGa-2. Qualitatively, this trend paralleled the content of the HOK phase (37, 18, and 4%, respectively) determined by the analysis of the XRD patterns (Drits et al., 2021; Sakharov et al., 2016). The smallest amount of non-intercalated material was recorded at the lowest temperature studied (~20% in KGa-1b, 50% in Hywite, and 60% in KGa-2, at 5°C). The interlayer acted as a sink for NMF which, once intercalated at some low temperature in a closed system, could not deintercalate upon increasing temperature. Intercalation capacity should not, therefore, be used to characterize kaolinite without reference to both intercalation temperature and thermal history.

The unusual effect of temperature and its dependence on the type of kaolinite could not be attributed to differences in the interlayer energetics of the three systems investigated. The interlayer bonding of the intercalated phases, as probed by the position and width of the $2\nu_{\text{NH}}$ mode of intercalated NMF, was independent of kaolinite type, reaction progress, and thermal history. It was, therefore, concluded that the intercalation capacity depends on the edges of the crystallites offering docking sites for NMF. A critical number of such edge-adsorbed NMF molecules is required to create the “wedge effect” described by Weiss et al. (1981). It is reasonable to assume a link between the layer stacking pattern in a kaolinite particle and the exact structure of its edges. It is also reasonable to assume that the sticking coefficient of NMF to these sites may be decreasing with increasing temperature. Unfortunately, these edges are the least known part of

the structure because they are not observed directly by either XRD or spectroscopic techniques.

Testing the aforementioned working hypothesis requires research focused on the chemical structure of the crystallite edges. The role of stacking translations and their sequence in the structure of the edges needs to be sought explicitly. Systematic studies of intercalation capacity need to be extended to kaolinites which are more ordered than KGa-1b. The present work was based on pre-dried kaolinite and NMF; the pioneering work of Olejnik et al. (1968, 1970) has indicated, however, that the concentration of H₂O in the surrounding NMF fluid can have a non-monotonic effect on the kinetics of intercalation. The competitive or synergetic role of H₂O on edge adsorption also deserves further study.

Acknowledgments Marek Szczerba (PAS) and Vassilis Gionis (NHRF) are thanked for helpful discussions. FA acknowledges the financial support from the project 'Advanced Materials and Devices' (MIS 5002409) of TPCI/NHRF which was implemented under the 'Action for the Strategic Development on the Research and Technological Sector,' funded by the Operational Program 'Competitiveness, Entrepreneurship and Innovation' (NSRF 2014–2020) and co-financed by Greece and the European Union (European Regional Development Fund). AD acknowledges the support from the National Science Centre, Poland (grant 25/B/ST10/01675). All other work at NHRF was supported with funds from the Applied Spectroscopy Laboratory of TPCI.

Funding Open access funding provided by HEAL-Link Greece.

Data availability Data included in the manuscript are available upon request.

Code availability N/a.

Declarations

Full details regarding funding are provided in the acknowledgement section.

Conflicts of interest The authors declare that they have no conflicts of interest.

Open Access This article is licensed under a Creative Commons Attribution 4.0 International License, which permits use, sharing, adaptation, distribution and reproduction in any medium or format, as long as you give appropriate credit to the original author(s) and the source, provide a link to the Creative Commons licence, and indicate if changes were made. The images or other third party material in this article are included in the article's Creative Commons licence, unless indicated otherwise in a credit line to the material. If material is not included in the article's Creative Commons licence and your intended use is not permitted by statutory regulation or exceeds

the permitted use, you will need to obtain permission directly from the copyright holder. To view a copy of this licence, visit <http://creativecommons.org/licenses/by/4.0/>.

References

- Adams, J. M. (1978). Differential Scanning Calorimetric Study of the Kaolinite: N-Methylformamide Intercalate. *Clays and Clay Minerals*, 26(2), 169–172. <https://doi.org/10.1346/CCMN.1978.0260213>
- Adams, J. M. (1979). The crystal structure of a dickite: N-methylformamide Intercalate [Al₂Si₂O₅(OH)₄:HCONHCH₃]. *Acta Crystallographica*, B35(5), 1084–1088. <https://doi.org/10.1107/S0567740879005628>
- Andreou, F. T., Barylska, B., Ciesielska, Z., Szczerba, M., Derkowski, A., Siranidi, E., Gionis, V., & Chryssikos, G. D. (2021). Intercalation of N-methylformamide in kaolinite: In situ monitoring by near-infrared spectroscopy and X-ray diffraction. *Applied Clay Science*, 212, 106209. <https://doi.org/10.1016/j.clay.2021.106209>
- Chryssikos, G. D., & Gates, W. P. (2017). Spectral manipulation and introduction to multivariate analysis. In W. P. Gates, J. T. Klopogge, J. Madejová, & F. Bergaya (Eds.), *The Application of Vibrational Spectroscopy to Clay Minerals and Layered Double Hydroxides* (Developments in Clay Science, Volume 8, Chapter 4) (pp. 64–106). <https://doi.org/10.1016/B978-0-08-100355-8.00004-7>
- Dedzo, G. K., & Detellier, C. (2016). Functional nanohybrid materials derived from kaolinite. *Applied Clay Science*, 130, 33–39. <https://doi.org/10.1016/j.clay.2016.01.010>
- Deng, Y., White, G. N., & Dixon, J. B. (2002). Effect of structural stress on the intercalation rate of kaolinite. *Journal of Colloid and Interface Science*, 250(2), 379–393. <https://doi.org/10.1006/jcis.2001.8208>
- Drits, V. A., Sakharov, B. A., Dorzhieva, O. V., Zviagina, B. B., & Lindgreen, H. (2019). Determination of the phase composition of partially dehydroxylated kaolinites by modelling their X-ray diffraction patterns. *Clay Minerals*, 54(3), 309–322. <https://doi.org/10.1180/clm.2019.39>
- Drits, V. A., Zviagina, B. B., Sakharov, B. A., Dorzhieva, O. V., & Savichev, A. T. (2021). New insight into the relationships between structural and FTIR spectroscopic features of kaolinites. *Clays and Clay Minerals*, 69(3), 366–388. <https://doi.org/10.1007/s42860-021-00133-w>
- Fashina, B., & Deng, Y. (2021). Stacking disorder and reactivity of kaolinites. *Clays and Clay Minerals*, 69(3), 354–365. <https://doi.org/10.1007/s42860-021-00132-x>
- Frost, R. L., Kristóf, J., Horvath, E., & Klopogge, J. T. (1999). Deintercalation of dimethylsulphoxide intercalated kaolinites - a DTA/TGA and Raman spectroscopic study. *Thermochimica Acta*, 327(1–2), 155–166. [https://doi.org/10.1016/S0040-6031\(98\)00605-4](https://doi.org/10.1016/S0040-6031(98)00605-4)
- Frost, R. L., Kristóf, J., Horvath, E., & Klopogge, J. T. (2000). Effect of water on the formamide-intercalation of kaolinite. *Spectrochimica Acta Part A: Molecular and Biomolecular Spectroscopy*, 56(9), 1711–1729. [https://doi.org/10.1016/s1386-1425\(00\)00224-9](https://doi.org/10.1016/s1386-1425(00)00224-9)

- Frost, R. L., van der Gaast, S. J., Zbik, M., Klopogge, J. T., & Paroz, G. N. (2002). Birdwood kaolinite: A highly ordered kaolinite that is difficult to intercalate – an XRD, SEM and Raman spectroscopic study. *Applied Clay Science*, 20(4–5), 177–187. [https://doi.org/10.1016/S0169-1317\(01\)00071-0](https://doi.org/10.1016/S0169-1317(01)00071-0)
- Gomes, C.S.F. (1982). Relação entre capacidade de intercalação de caulinites e defeitos estruturais. Boletim da Sociedade Geologica de Portugal, XXIII, 55-64.
- Hach-Ali, P.F., & Weiss, A. (1969). Estudio de la reaccion de caolinita y N-metilformamida. *Quimica LXV*, 769-790.
- Klopogge, J. T. (2019). Intercalation of the kaolin minerals with simple molecules. In J. T. Klopogge (Ed.), *Spectroscopic Methods in the Study of Kaolin Minerals and Their Modifications* (pp. 243–319). Springer. https://doi.org/10.1007/978-3-030-02373-7_6
- Kovács, A., & Makó, É. (2016). Cooling as the key parameter in formation of kaolinite ammonium acetate and halloysite-ammonium acetate complexes using homogenization method. *Colloids and Surfaces A: Physicochemical and Engineering Aspects*, 508(5), 70–78. <https://doi.org/10.1016/j.colsurfa.2016.08.025>
- Kristóf, J., Frost, R. L., Klopogge, J. T., Horvath, E., & Gábor, M. (1999). Thermal behavior of kaolinite intercalated with formamide, dimethyl sulphoxide and hydrazine. *Journal of Thermal Analysis and Calorimetry*, 56(2), 885–891. <https://doi.org/10.1023/a:1010139113778>
- Lagaly, G. (1984). Clay organic interactions. *Philosophical Transactions of the Royal Society A: Mathematical, Physical and Engineering Sciences*, 311(1517), 315–332. <https://doi.org/10.1098/rsta.1984.0031>
- Lagaly, G., Ogawa, M., & Dékány, I. (2006). Clay Mineral Organic Interactions. In F. Bergaya, B. K. G. Theng, & G. Lagaly (Eds.), *Handbook of Clay Science* (pp. 309–377). Elsevier. [https://doi.org/10.1016/S1572-4352\(05\)01010-X](https://doi.org/10.1016/S1572-4352(05)01010-X)
- Makó, É., Kovács, A., & Kristóf, T. (2019). Influencing parameters of direct homogenization intercalation of kaolinite with urea, dimethyl sulfoxide, formamide, and N-methylformamide. *Applied Clay Science*, 182, 105287. <https://doi.org/10.1016/j.clay.2019.105287>
- Olejnik, S., Aylmore, L. A. G., Posner, A. M., & Quirk, J. P. (1968). Infrared spectra of kaolin mineral-dimethyl sulfoxide complexes. *The Journal of Physical Chemistry A*, 72(1), 241–249. <https://doi.org/10.1021/j100847a045>
- Olejnik, S., Posner, A. M., & Quirk, J. P. (1970). The intercalation of polar organic compounds into kaolinite. *Clay Minerals*, 8(4), 421–434. <https://doi.org/10.1180/claymin.1970.008.4.05>
- Olejnik, S., Posner, A. M., & Quirk, J. P. (1971a). The I.R. spectra of interlamellar kaolinite-amide complexes I. The complexes of formamide, N-methyl formamide and dimethylformamide. *Clays and Clay Minerals*, 19(2), 83–94. <https://doi.org/10.1346/CCMN.1971.0190204>
- Olejnik, S., Posner, A. M., & Quirk, J. P. (1971b). The infrared spectra of interlamellar kaolinite-amide complexes II. Acetamide, N-methylacetamide and dimethylacetamide. *Journal of Colloid and Interface Science*, 37(3), 536–547. [https://doi.org/10.1016/0021-9797\(71\)90331-6](https://doi.org/10.1016/0021-9797(71)90331-6)
- Rausell-Colom, J. A., & Serratos, J. M. (1987). Reactions of Clays with Organic Substances. In A. C. D. Newman (Ed.), *Chemistry of Clays and Clay Minerals* (pp. 371–422). Longman Scientific & Technical.
- Ruiz Cruz, M. D., & Franco, F. (2000). Thermal Behavior of the Kaolinite-Hydrazine Intercalation Complex. *Clays and Clay Minerals*, 48(1), 63–67. <https://doi.org/10.1346/CCMN.2000.480108>
- Sakharov, B. A., Drits, V. A., McCarty, D. K., & Walker, G. M. (2016). Modeling Powder X-Ray Diffraction Patterns of the Clay Minerals Society Kaolinite Standards: Kga-1, Kga-1b, and Kga-2. *Clays and Clay Minerals*, 64(3), 314–333. <https://doi.org/10.1346/CCMN.2016.0640307>
- Seifi, S., Diatta-Dieme, M. T., Blanchart, P., Lecomte-Nana, G. L., Kobor, D., & Petit, S. (2016). Kaolin intercalated by urea. Ceramic applications. *Construction and Building Materials*, 113, 579–585. <https://doi.org/10.1016/j.conbuilmat.2016.03.095>
- Tunney, J. J., & Detellier, C. (1996). Chemically modified kaolinite. Grafting of methoxy groups on the interlamellar aluminol surface of kaolinite. *Journal of Materials Chemistry*, 6(10), 1679–1685. <https://doi.org/10.1039/JM9960601679>
- Uwins, P. J. R., Mackinnon, I. D. R., Thompson, J. G., & Yago, A. J. E. (1993). Kaolinite: NMF intercalates. *Clays and Clay Minerals*, 41(6), 707–717. <https://doi.org/10.1346/CCMN.1993.0410609>
- Weiss, A., Becker, H. O., Orth, H., Mai, G., Lechner, H., & Range, K. J. (1970). Particle Size Effects and Reaction Mechanism of the Intercalation into Kaolinite. In L. Heller (Ed.), *Proceedings of International Clay Conference* (pp. 180–184). Israel University Press.
- Weiss, A., Choy, J. H., Meyer, H., & Becker, H. O. (1981). Hydrogen reorientation, a primary step of intercalation reactions into kaolinite. In H. Van Olphen & F. Veniale (Eds.), *Proceedings of International Clay Conference* (p. 331). Elsevier.
- Xie, X., & Hayashi, S. (1999). NMR study of kaolinite intercalation compounds with formamide and its derivatives. 1. Structure and orientation of guest molecules. *The Journal of Physical Chemistry B*, 103(29), 5949–5955. <https://doi.org/10.1021/jp9902371>
- Zhang, S., Ou, X., Qiang, Y., Niu, J., & Komarneni, S. (2015). Thermal decomposition behavior and de-intercalation mechanism of acetamide intercalated into kaolinite by thermoanalytical techniques. *Applied Clay Science*, 114, 309–314. <https://doi.org/10.1016/j.clay.2015.06.002>
- Zhang, S., Liu, Q., Gao, F., Li, X., Liu, C., Li, H., Boyd, S. A., Johnston, C. T., & Teppen, B. J. (2017). Mechanism Associated with Kaolinite Intercalation with Urea: Combination of Infrared Spectroscopy and Molecular Dynamics Simulation Studies. *Journal of Physical Chemistry C*, 121(1), 402–409. <https://doi.org/10.1021/acs.jpcc.6b10533>